Analytical Study of Heat Transfer under Effect of Internal Heat Generation and Radiation over a Stretching Surface

M. Almas[1,2,*]

[1]Department of Mechanical and Materials Engineering, Florida International University, Miami, FL 33199, USA

[2]Department of Marine engineering, King Abdulaziz University, 21589, Saudi Arabia

Abstract: Homotopy Analysis Method (HAM) is used to analytically study the heat transfer in a porous medium over a stretching surface with internal heat generation and radiation. The governing equations are transformed into a system of ordinary differential equations and then solved using HAM method. Effects of different physical parameters such as permeability, suction, Prandtl number, radiation and Heat generation have been studied on temperature and velocity fields. And also analytical results have been shown for local skin friction coefficient and the Nusselt number. The analytical solutions have been compared with numerical results which showed remarkable agreements.

Keywords: Homotopy analysis method (HAM), numerical method (NM), porous medium, suction and injection, internal heat generation.

1. INTRODUCTION

Boundary layer flows on continuous moving surface have many engineering applications. Cooling of an infinite metallic plate in a cooling bath, aerodynamic extrusion of plastic sheets, the boundary layer along a liquid film in condensation processes and a polymer sheet or filament extruded continuously from a dye, or a long thread traveling between a feed roll and a windup roll, are examples for practical applications of continuous flat surface. Sriramula *et al*. [1] investigated the flow and heat transfer of a viscous incompressible flow in porous medium over a stretching sheet studied. Subhas and Veena [2] studied the Visco-elastic fluid flow and heat transfer in a saturated porous medium over an impermeable stretching surface. Elbashbeshy and Bazid [3-5] analyzed heat transfer over continuously moving plate embedded in non-Darcian porous medium. They studied heat transfer over unsteady stretching surface with internal heat generation or absorption. Pop and Na [6] studied free convection heat transfer of non-Newtonian fluids along a vertical wavy surface in a porous medium. Most of engineering problems, especially heat transfer equations are mostly nonlinear. There are many effective methods for obtaining the solutions of nonlinear equation such as, variational iteration method [7], Adomian method [8] and Homotopy perturbation method [9-10], and HAM [11-21]. HAM expresses solutions of a nonlinear problem by means of different base functions and unlike perturbation techniques, it is independent of any small or large quantities.

In this study Homotopy Analysis Method has been implemented to study boundary layer [22-31] heat transfer in a porous medium over a stretching surface in the presence of internal heat generation and radiation.

2. GOVERNING EQUATION

In this study a steady, incompressible and 2-D laminar viscous flow through a porous medium over a stretching surface with a uniform wall with negligible radiative heat flux in the *x* -direction temperature has been considered. The conservation equations of the laminar boundary layer are as follows:

$$\frac{\partial u}{\partial x}+\frac{\partial v}{\partial y}=0 \tag{1}$$

$$\rho\left(u\frac{\partial u}{\partial x}+v\frac{\partial u}{\partial y}\right)=\mu\frac{\partial^2 u}{\partial y^2}-\frac{\mu_e}{K'}u \tag{2}$$

$$u\frac{\partial T}{\partial x}+v\frac{\partial T}{\partial y}=\alpha_c\frac{\partial^2 T}{\partial y^2}+Q(T-T_\infty)-\frac{1}{\rho c_p}\frac{\partial q_r}{\partial y} \tag{3}$$

where, u, v are the velocity components along x, y coordinates respectively, ρ is the density of the fluid, K' is the permeability of the porous medium, μ is the coefficient of the dynamic viscosity, μ_e is the effective viscosity, T is the temperature of the fluid in the

*Address correspondence to this author at the Department of Mechanical and Materials Engineering, Florida International University, Miami, FL 33199, USA; Tel: 7862103780; Fax: 00966126952437; E-mail: majidaaia@gmail.com

E-ISSN: 2409-5761/15

boundary layer, T_∞ is the temperature of the fluid outside the boundary layer, α_c is the effective thermal diffusivity of the saturated porous medium and Q is the volumetric rate of heat generation.

$$q_r = -\frac{4\sigma_1}{3\kappa_1}\frac{\partial T^4}{\partial y} \tag{4}$$

where σ_1 is the Stefan-Boltzmann constant and κ_1 is the mean absorption coefficient. We assume that the temperature differences within the flow are sufficiently small such that T4 may be expressed as a linear function of temperature. This is accomplished by expanding T^4 in a Taylor's series about T_∞ and neglecting higher-order terms, thus

$$T^4 \cong T_\infty^{\ 4} + (T - T_\infty)\times 4T_\infty^{\ 3} = 4T_\infty^{\ 3}T - 3T_\infty^{\ 4} \tag{5}$$

By using of Eqs. (4) and (5), Eq. (3) gives

$$u\frac{\partial T}{\partial x} + v\frac{\partial T}{\partial y} = \frac{\kappa}{\rho c_p}\frac{\partial^2 T}{\partial y^2} + Q(T - T_\infty) + \frac{16\sigma_1 T_\infty^{\ 3}}{3\rho c_p \kappa_1}\frac{\partial^2 T}{\partial y^2} \tag{6}$$

The corresponding boundary conditions for the above problem are given by

$$u = u_0 x, v = \pm v_w, T = T_w \text{ at } y = 0 \tag{7}$$

$$u = 0, T = T_\infty \text{ as } y \to \infty \tag{8}$$

Positive and negative values for v_w indicate blowing and suction respectively, while $v_w = 0$ corresponds to an impermeable plate.

The following non-dimensional variables are introduced in order to obtain the non-dimensional governing equations:

$$\eta = y\sqrt{\frac{u_0\rho}{\mu}}, \psi(x,y) = \sqrt{\frac{\mu u_0}{\rho}}xf(\eta), \theta = \frac{T - T_\infty}{T_w - T_\infty} \tag{9}$$

where, ψ is the stream function.

Since $u = \frac{\partial \psi}{\partial y}$ and $v = -\frac{\partial \psi}{\partial x}$, we have from Eq. (9) that

$$u = u_0 x f'(\eta) \text{ and } v = -\sqrt{\frac{\mu u_0}{\rho}}f(\eta) \tag{10}$$

Here f is non-dimensional stream function and prime denotes differentiation with respect to η. Now by substituting Eqs. (9) and (10) into Eqs. (1), (2) and (6) we obtain,

$$\begin{cases} f''' + ff'' - f'^2 - Kf' = 0 \\ \theta'' + Pn(\lambda\theta + f\theta') = 0 \end{cases} \tag{11}$$

where $K = \frac{\mu_e}{\rho K' u_0}$ is the permeability parameter, $\lambda = \frac{Q}{u_0}$ is the heat generation or absorption parameter, $Pn = \frac{3N\,\mathrm{Pr}}{3N + 4}$ is the radiative Prandtl number, $N = \frac{\kappa\kappa_1}{4\sigma_1 T_\infty^{\ 3}}$ is the radiation parameter, $\mathrm{Pr} = \frac{\rho \upsilon_a c_p}{\kappa}$ is the Prandtl number.

The corresponding boundary conditions (7) and (8) becomes,

$$\begin{cases} f(0) = f_w, f'(0) = 1 \\ \theta(0) = 1 \end{cases}, \begin{cases} f'(\infty) = 0 \\ \theta(\infty) = 0 \end{cases} \tag{12}$$

where $f_w = \mp v_w\sqrt{\frac{\rho}{\mu u_0}}$ is the suction and injection velocity at the plate for $f_w > 0$ and $f_w < 0$ respectively.

The quantities of main interest in such problem are the skin friction coefficient and the Nusselt number (rate of heat transfer). The shearing stress on the surface is defined by

$$\tau_w = \mu\left(\frac{\partial u}{\partial y}\right)_{y=0} \tag{13}$$

$$c_f = \frac{\tau_w}{\frac{1}{2}\rho u_0^{\ 2}} = 2x^{3/2}\,\mathrm{Re}_x^{-1/2}\, f''(0) \tag{14}$$

where $\mathrm{Re}_x = \frac{u_0 x}{\upsilon_a}$ is local Reynolds number.

Thus from Eq. (14) we see that the local values of the skin friction coefficient c_f is proportional to $f''(0)$. The heat flux on the wall can be defined as:

$$q_w(x) = \kappa\left(\frac{\partial T}{\partial y}\right)_{y=0} \tag{15}$$

$$h(x)=\frac{q_w(x)}{T_w-T_\infty} \quad (16)$$

The local Nusselt number may be written as

$$Nu=\frac{h(x)}{\kappa}=-(\mathrm{Re}_x)^{1/2}\theta'(0) \quad (17)$$

Thus from Eq. (17) we see that the local Nusselt number Nu is proportional to $-\theta'(0)$.

3. HOMOTOPY ANALYSIS METHOD SOLUTION

A solution may be expressed with different base functions, among which some converge to the exact solution of the problem faster than others. Such base functions are obviously better suited in terms of converging to the final solution. Noting these facts, $g(\eta)$ by a set of base functions is:

$$f(\eta)=\sum_{m=0}^{\infty}\sum_{n=0}^{\infty}\sum_{k=0}^{\infty}b_{m,n}^{k}\eta^{k}\exp(-n\eta), \quad (18)$$

$$\theta(\eta)=\sum_{m=0}^{\infty}\sum_{n=0}^{\infty}\sum_{k=0}^{\infty}b_{m,n}^{k}\eta^{k}\exp(-n\eta), \quad (19)$$

the initial guess and auxiliary linear operators are as follows:

$$f_0(\eta)=f_w+1-\exp(-\eta),\ \ \theta_0(\eta)=\exp(-\eta) \quad (20)$$

$$\mathcal{L}_1(f)=f'''+f'',\ \ \mathcal{L}_2(\theta)=\theta''+\theta' \quad (21)$$

$$\mathcal{L}_1(c_1+c_2\eta+c_3\exp(-\eta))=0,\ \ \mathcal{L}_2(c_4+c_5\exp(-\eta))=0 \quad (22)$$

where $c_i(i=1-5)$ are constants. Let $P\in[0,1]$ denotes the embedding parameter and $\hbar$ indicates non–zero auxiliary parameters. Then, we construct the following equations:

3.1. Zeroth –Order Deformation Equations

$$(1-P)\mathcal{L}_1\left[f(\eta;p)-f_0(\eta)\right]=p\hbar_1H(\eta)N_1\left[f(\eta;p)\right] \quad (23)$$

$$f(0;p)=f_w;\qquad f'(0;p)=1,\qquad f'(\infty;p)=0 \quad (24)$$

$$(1-P)\mathcal{L}_2\left[\theta(\eta;p)-\theta_0(\eta)\right]=p\hbar_2H(\eta)N_2\left[\theta(\eta;p)\right] \quad (25)$$

$$\theta(0;p)=1;\qquad \theta(\infty;p)=0 \quad (26)$$

$$N_1[f(\eta;p),\theta(\eta;p)]=\frac{\partial^3 f(\eta;p)}{\partial\eta^3}+ f(\eta;p)\frac{\partial^2 f(\eta;p)}{\partial\eta^2}-\left(\frac{\partial f(\eta;p)}{\partial\eta}\right)^2-K\frac{\partial f(\eta;p)}{\partial\eta} \quad (27)$$

$$N_2[f(\eta;p),\theta(\eta;p)]=\frac{\partial^2\theta(\eta;p)}{\partial\eta^2}+ Pn\left(\lambda\theta(\eta;p)+f(\eta;p)\frac{\partial\,\theta(\eta;p)}{\partial\eta}\right) \quad (28)$$

For $p=0$ and $p=1$ we have

$$f(\eta;0)=f_0(\eta)\qquad f(\eta;1)=f(\eta) \quad (29)$$

$$\theta(\eta;0)=\theta_0(\eta)\qquad \theta(\eta;1)=\theta(\eta) \quad (30)$$

when p increases from 0 to 1 then $f(\eta;p)$ and $\theta(\eta;p)$ vary from $f_0(\eta)$ and $\theta_0(\eta)$ to $f(\eta)$ and $\theta(\eta)$. By Taylor's theorem and using equation (29) and (30), we can write:

$$f(\eta;p)=f_0(\eta)+\sum_{m-1}^{\infty}f_m(\eta)p^m,\ \ f_m(\eta)=\frac{1}{m!}\frac{\partial^m(f(\eta;p))}{\partial p^m} \quad (31)$$

$$\theta(\eta;p)=\theta_0(\eta)+\sum_{m-1}^{\infty}\theta_m(\eta)p^m,\ \ \theta_m(\eta)=\frac{1}{m!}\frac{\partial^m(\theta(\eta;p))}{\partial p^m} \quad (32)$$

In which $\hbar_1$ and $\hbar_2$ are chosen in such a way that these two series are convergent at $p=1$, therefore we have through equation (31) and (32):

$$f(\eta)=f_0(\eta)+\sum_{m=1}^{\infty}f_m(\eta), \quad (33)$$

$$\theta(\eta)=\theta_0(\eta)+\sum_{m=1}^{\infty}\theta_m(\eta) \quad (34)$$

3.2. mth–Order Deformation Equations

$$\mathcal{L}_1\left[f_m(\eta)-\chi_m f_{m-1}(\eta)\right]=\hbar_1H(\eta)R_m^f(\eta) \quad (35)$$

$$f_m(0)=0;\qquad f'_m(0)=0,\qquad f'_m(\infty)=0 \quad (36)$$

$$R_m^f(\eta)=f'''_{m-1}+\sum_{k=0}^{m-1}f_kf''_{m-1-k}-\sum_{k=0}^{m-1}f'_kf'_{m-1-k}-Kf'_{m-1} \quad (37)$$

$$\mathcal{L}_2\left[\theta_m(\eta)-\chi_m\theta_{m-1}(\eta)\right]=\hbar_2H(\eta)R_m^\theta(\eta) \quad (38)$$

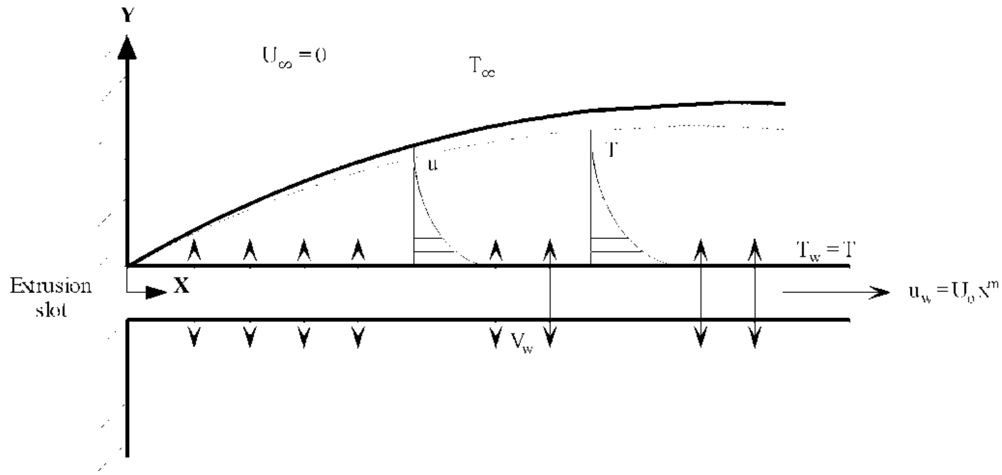

Figure 1: Schematic diagram of problem.

$$\theta_m(0) = 0; \qquad \theta_m(\infty) = 0 \tag{39}$$

$$R_m^\theta(\eta) = \theta''_{m-1} + Pn\left(\lambda\theta_{m-1-k} + \sum_{k=0}^{m-1} f_k \theta'_{m-1-k}\right) \tag{40}$$

$$\chi_m = \begin{cases} 0 & m \le 1 \\ 1 & m > 1 \end{cases} \tag{41}$$

The general solutions of Eqs. (35)-(40) are:

$$f_m(\eta) - \chi_m f_{m-1}(\eta) = f_m^*(\eta) + C_1^m + C_2^m \eta + C_3^m \exp(-\eta) \tag{42}$$

$$\theta_m(\eta) - \chi_m \theta_{m-1}(\eta) = \theta_m^*(\eta) + C_4^m + C_5^m \exp(-\eta) \tag{43}$$

Where C_1^m to C_5^m are constants that can be obtained by applying the boundary condition in Eq. (36) and (39).

As discussed in [11] the rule of coefficient ergodicity and the rule of solution existence play important roles in determining the auxiliary function and ensuring that the high-order deformation equations are closed and have solutions. Thus, the auxiliary function $H(\eta)$ is as follow:

$$H(\eta) = \exp(-\eta) \tag{44}$$

4. CONVERGENCE OF THE HAM SOLUTION

As stated in [11], the convergence and rate of approximation for the HAM solution strongly depends on the value of auxiliary parameter $\hbar$. By means of the so-called $\hbar$-curves it is easy to find out the so-called valid regions of $\hbar$ to gain a convergent solution series. According to Figure **2** and **3**, the acceptable range of auxiliary parameters for $pr = 0.73, K = 0.5,$ $\lambda = 0.03, N = 0.1$ are $-1.2 < \hbar_1 < -0.5$ and $-1.3 < \hbar_2 < -0.6$.

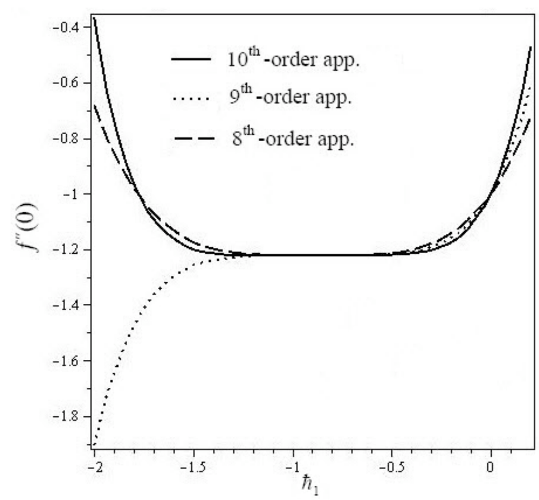

Figure 2: The $\hbar_1$-validity for $K = 0.5$, $\Pr = 0.73$, $N = 0.1$, $\lambda = 0.03$, $f_w = 0$.

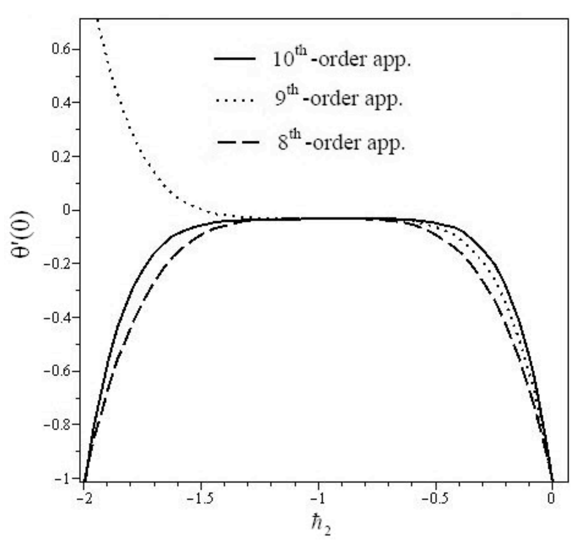

Figure 3: The $\hbar_1$-validity for $K = 0.5$, $\Pr = 0.73$, $N = 0.1$, $\lambda = 0.03$, $f_w = 0$.

Figure **4** and **5** shows how auxiliary parameters $\hbar_1$ and $\hbar_2$ varies with changing f_w. If f_w increases the range of convergence of solution is restricted and then decreased.

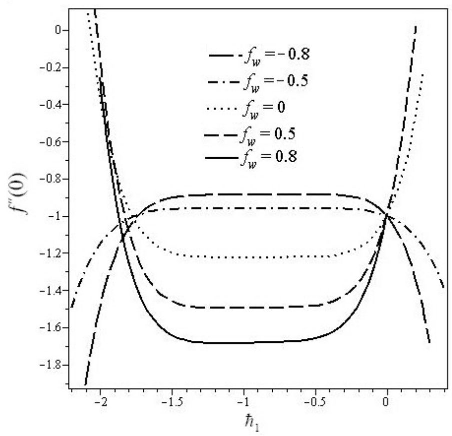

Figure 4: The $\hbar_1$-validity for various f_w, $K = 0.5$, $\Pr = 0.73$, $N = 0.1$, $\lambda = 0.03$.

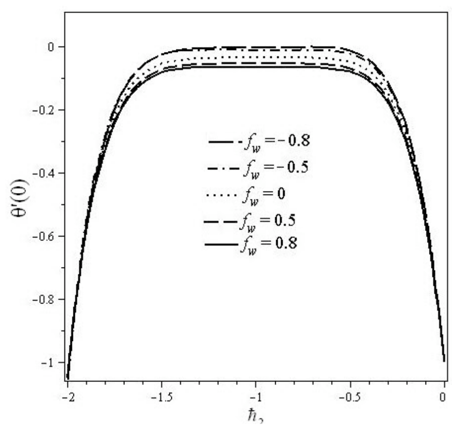

Figure 5: The $\hbar_2$-validity for various f_w, $K = 0.5$, $\Pr = 0.73$, $N = 0.1$, $\lambda = 0.03$.

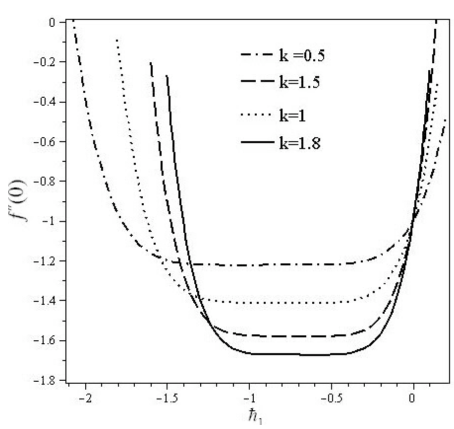

Figure 6: The $\hbar_1$-validity for various K, $f_w = 0$, $\Pr = 0.73$, $N = 0.1$, $\lambda = 0.03$.

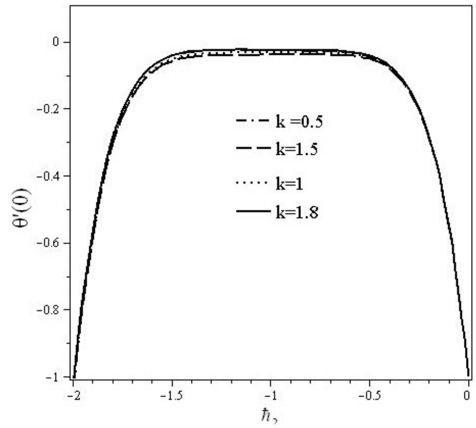

Figure 7: The $\hbar_2$-validity for various K, $f_w = 0$, $\Pr = 0.73$, $N = 0.1$, $\lambda = 0.03$.

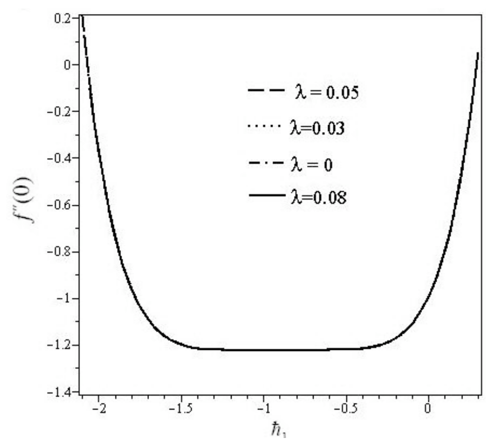

Figure 8: The $\hbar_1$- validity for various λ, $f_w = 0$, $\Pr = 0.73$, $N = 0.1$, $K = 0.5$.

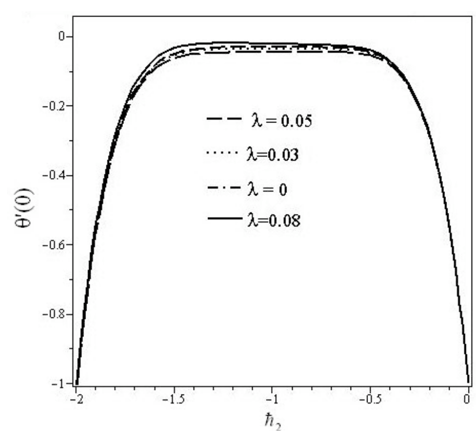

Figure 9: The $\hbar_2$-validity for various λ, $f_w = 0$, $\Pr = 0.73$, $N = 0.1$, $K = 0.5$.

5. RESULTS AND DISCUSSION

In the calculations, the values of permeability parameter *K*, suction parameter f_w, Prandtl number *Pr*,

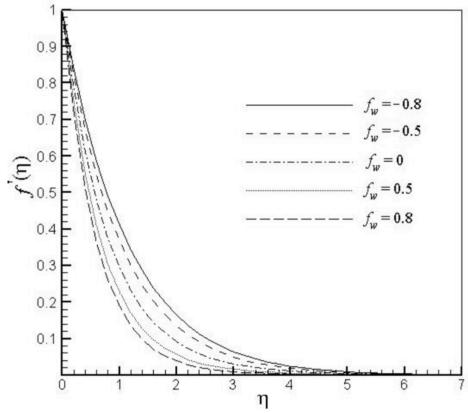

Figure 10: Velocity profile f' for various f_w when $\Pr = 0.73$, $N = 0.1$, $K = 0.5$, $\lambda = 0.03$.

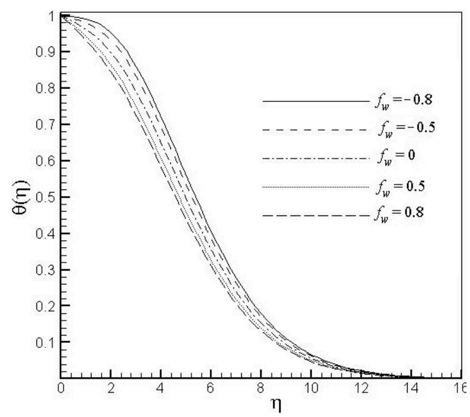

Figure 11: Temperature profile θ' for various f_w when $\Pr = 0.73$, $N = 0.1$, $K = 0.5$, $\lambda = 0.03$.

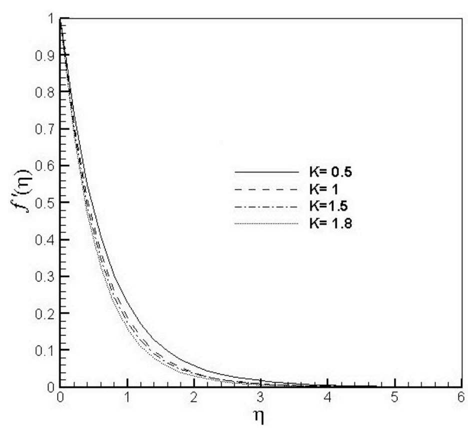

Figure 12: Velocity profile f' for various K when $\Pr = 0.73$, $N = 0.1$, $f_w = 0.5$, $\lambda = 0.03$.

radiation parameter *N*, Heat generation or absorption parameter λ are chosen arbitrarily. Figure **10** shows the dimensionless velocity profiles for different values of injection and suction parameters f_w. It can be seen that the velocity profiles decrease monotonically with the increase of injection parameter as well as suction parameter. Figure **11** also shows the similar behavior (like as the velocity profiles) of the effect of suction and injection parameter on the temperature profiles. Figures **12** and **14** show the velocity profiles for different values of permeability parameter K in case of suction and injection. From these figures, we see that the velocity decreases with the increase of the permeability parameter K in both case of suction and injection.

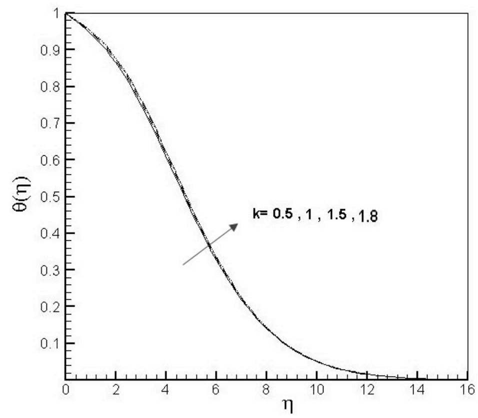

Figure 13: Temperature profile θ' for various K when $\Pr = 0.73$, $N = 0.1$, $f_w = 0.5$, $\lambda = 0.03$.

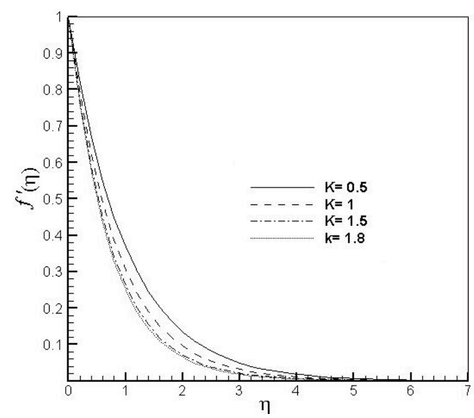

Figure 14: Velocity profile f' for various K when $\Pr = 0.73$, $N = 0.1$, $f_w = -0.5$, $\lambda = 0.03$.

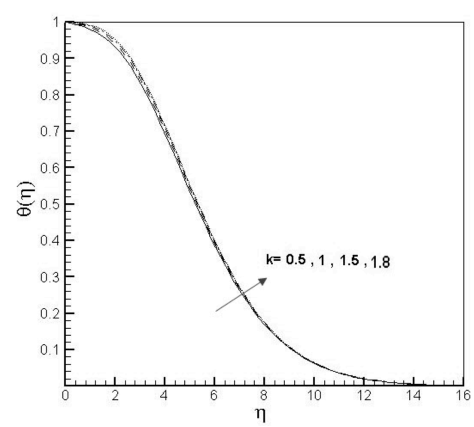

Figure 15: Temperature profile θ' for various K when $\Pr = 0.73$, $N = 0.1$, $f_w = -0.5$, $\lambda = 0.03$.

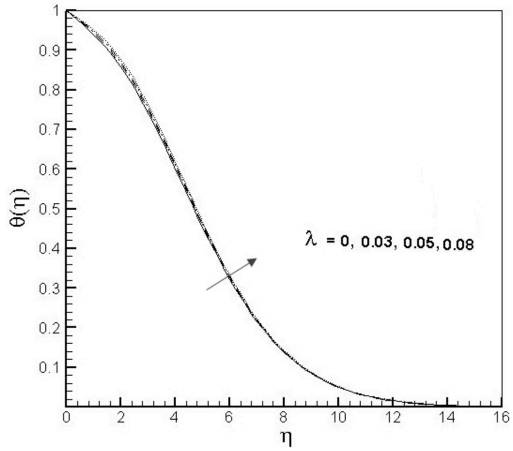

Figure 16: Temperature profile θ' for various λ when $\Pr = 0.73$, $N = 0.1$, $f_w = 0.5$, $K = 0.5$.

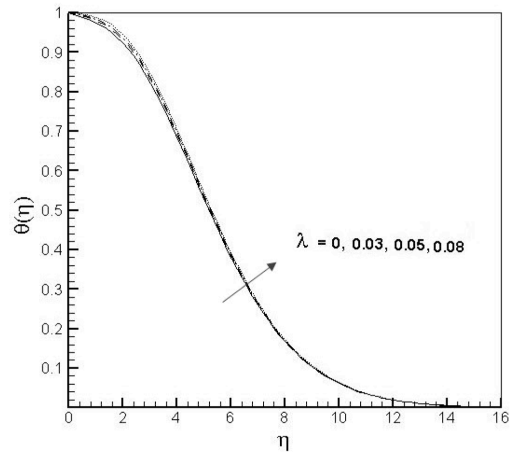

Figure 17: Temperature profile θ' for various λ when $\Pr = 0.73$, $N = 0.1$, $f_w = -0.5$, $K = 0.5$.

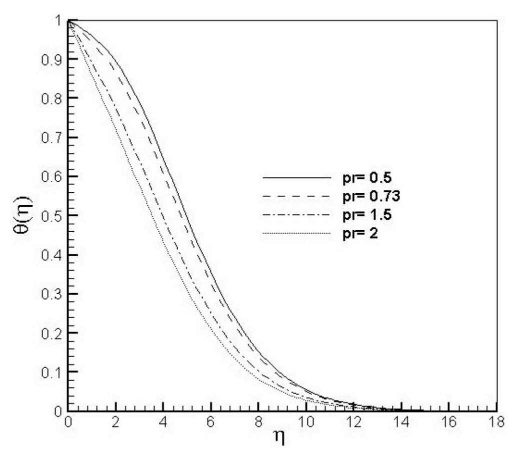

Figure 18: Temperature profile θ' for various $\Pr$ when $\lambda = 0.03$, $N = 0.1$, $f_w = 0.5$, $K = 0.5$.

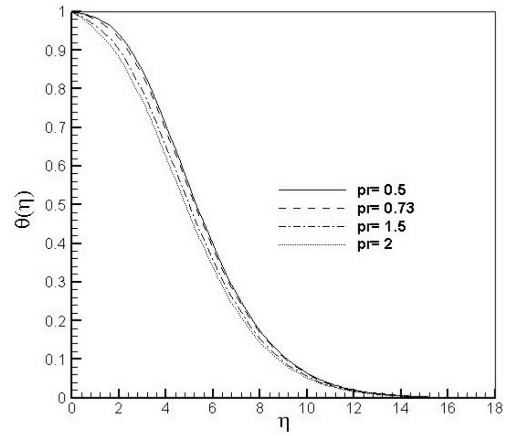

Figure 19: Temperature profile θ' for various $\Pr$ when $\lambda = 0.03$, $N = 0.1$, $f_w = -0.5$, $K = 0.5$.

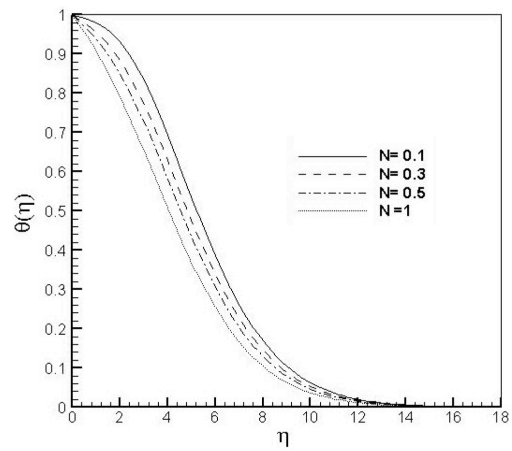

Figure 20: Temperature profile θ' for various N when $\lambda = 0.03$, $\Pr = 0.73$, $f_w = 0.5$, $K = 0.5$.

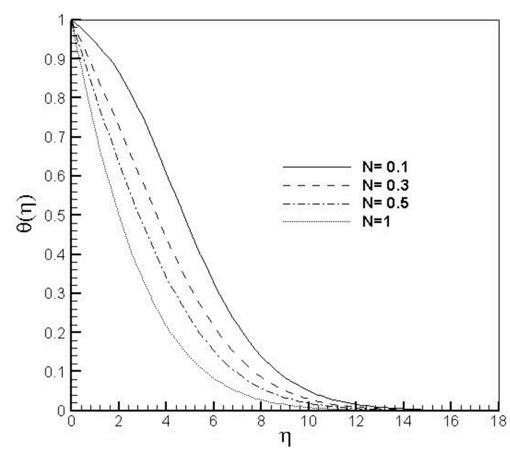

Figure 21: Temperature profile θ' for various N when $\lambda = 0.03$, $\Pr = 0.73$, $f_w = -0.5$, $K = 0.5$.

Figures **18** and **19** show the temperature profiles for different values of Prandtl number Pr. From these figures we see that the dimensionless temperature profile decreases with increasing Pr in case of suction and injection. All the above calculations have been carried out for a fixed radiation parameter N. Therefore, the effects of radiation parameter N on velocity and temperature profiles are not clear from the earlier discussions. Figures **20** and **21** show the effect of radiation parameter N on the temperature profiles in the case of suction and injection. We observe from these figures that temperature profile decreases with the increase of radiation parameter for both cases. For large N, it is clear that temperature decreases more rapidly with the increase of N. Therefore using radiation, we can control the temperature distributions.

Table 1: The Results of HAM and NS for $f(\eta)$, $f'(\eta)$, $\theta(\eta)$ when $f_w = 0$, $\mathrm{Pr} = 0.73$, $\lambda = 0.03$, $\mathrm{N} = 0.1$, $\mathrm{K} = 0.5$

η	$f(\eta)$			$f'(\eta)$			$\theta(\eta)$		
	HAM	NS	Error (%)	HAM	NS	Error (%)	HAM	NS	Error (%)
0.0	0.0000	0.0000	0	0.9995	0.9999	0.0400	0.9998	0.9999	0.010
0.2	0.1747	0.1773	1.4664	0.7831	0.7827	0.05110	0.9904	0.9917	0.1310
0.4	0.3150	0.3162	0.37950	0.6131	0.6126	0.08161	0.9827	0.9835	0.0813
0.6	0.4261	0.4249	0.28241	0.4802	0.4795	0.14598	0.9748	0.9752	0.0410
0.8	0.5086	0.5099	0.25495	0.3757	0.3753	0.10658	0.9690	0.9668	0.227
1.0	0.5812	0.5765	0.81526	0.2942	0.2938	0.1361	0.9607	0.9585	0.2295
1.2	0.6296	0.6287	0.14315	0.2305	0.2299	0.2609	0.9531	0.9501	0.3157
1.4	0.6688	0.6695	0.10455	0.1805	0.1800	0.277	0.9450	0.9418	0.3397
1.6	0.6987	0.7014	0.3849	0.1410	0.1402	0.5706	0.9380	0.9334	0.4928
1.8	0.7272	0.7264	0.1101	0.1107	0.1103	0.36264	0.9317	0.9250	0.7243
2.0	0.7474	0.7460	0.18766	0.0863	0.0863	0	0.9175	0.9167	0.0872
2.2	0.7614	0.7613	0.01313	0.0675	0.0675	0	0.9112	0.9084	0.3082
2.4	0.7717	0.7733	0.20690	0.0530	0.0628	15.605	0.9002	0.9000	0.022
2.6	0.7790	0.7826	0.4600	0.0414	0.0414	0	0.8908	0.8917	0.101
2.8	0.7883	0.7900	0.21518	0.0326	0.0324	0.61728	0.8777	0.8834	0.6452
3.0	0.7973	0.7957	0.2010	0.0254	0.0253	0.3952	0.8699	0.8751	0.59421

Table 2: The Results of HAM and NS for $f''(0)$, $\theta'(0)$ when $f_w = -0.5$, $\mathrm{Pr} = 0.73$, $\lambda = 0.03$, $N = 0.1$, $K = 0.5$

K	$\hbar_1$	$\hbar_2$	$f''(0)$		$-\theta'(0)$	
			HAM	NS	HAM	NS
0.5	-1.0	-1.0	-1.0000	-0.9999	0.0294	0.0295
1.0	-0.9	-1.0	-1.1864	-1.1861	0.0250	0.0251
1.5	-0.8	-1.0	-1.3514	-1.3507	0.0223	0.0223

Table 3: The Results of HAM and NS for $f''(0)$, $\theta'(0)$ when $f_w = 0.5$, $\mathrm{Pr} = 0.73$, $\lambda = 0.03$, $\mathrm{N} = 0.1$, $\mathrm{K} = 0.5$

K	$\hbar_1$	$\hbar_2$	$f''(0)$		$-\theta'(0)$	
			HAM	NS	HAM	NS
0.5	-1.2	-1.0	-1.4994	-1.5000	0.0549	0.0551
1.0	-1.0	-1.0	-1.6854	-1.6860	0.0522	0.0523
1.5	-1.0	-1.0	-1.8520	-1.8507	0.0503	0.0504

Table 4: The Results of HAM and NS for $f''(0)$, $\theta'(0)$ for Various f_w When, $\mathrm{Pr}=0.73$, $\lambda=0.03$, $\mathrm{N}=0.1$, $\mathrm{K}=0.5$

Pr	$f''(0)$		$-\theta'(0)$	
	$f_w = -0.5$		$f_w = 0.5$	
	HAM	NS	HAM	NS
0.73	0.0293	0.0295	0.0549	0.0550
1.5	0.0270	0.0271	0.0955	0.0957
2.0	0.0268	0.0269	0.1282	0.1284

6. CONCLUSION

In this study, we have applied Homotopy Analysis Method (HAM) to compute heat transfer in a porous medium over a stretching surface with internal heat generation and suction or injection. Using usual similarity transformations, the governing equations have been transformed into a system of non-linear ordinary differential equations and are solved for similar solutions by using (HAM). The proper range of the auxiliary parameter $\hbar$ to ensure the convergency of the solution series was obtained through the so-called $\hbar$-curves. When compared with other analytic methods, it is clear that HAM provides highly accurate analytic solutions for nonlinear problems. A analytical study has been performed to survey the influence of permeability parameter, heat source (sink) parameter, Prandtl number and radiation parameter on the skin friction coefficient, the rate of heat transfer coefficient, dimensionless velocity and temperature profiles. From the above investigation, we found that Radiation has significant effect on temperature profiles. Velocity profiles decrease with increasing injection as well as suction. The temperature profiles increase with increasing permeability and heat source parameter and decreases with increasing Prandtl number and radiation parameter. The skin friction coefficient increases with heat source and decreases with permeability. The rate of heat transfer coefficient decreases with heat source parameter as well as permeability and increases with Prandtl number as well as radiation parameter. It has been attempted to show the accuracy, capabilities and wide-range applications of the homotopy analysis method in comparison with the numerical solution of nonlinear heat transfer in a porous medium over a stretching surface with internal heat generation and suction or injection.

ACKNOWLEDGMENTS

The author would like to thank both the Saudi Arabian Cultural Mission in Washington D.C. and King Abdulaziz University in Jeddah, KSA for their support.

NOMENCLATURE

B	Positive constant
f	Non-dimensional stream function
$\hbar$	Auxiliary parameter
HAM	Homotopy Analysis Method
H	Auxiliary function
$\mathcal{L}$	Linear operator of HAM
N	Non-linear operator/radiation parameter
a_c	Effective thermal diffusivity
Pr	Prandtl number
Pn	Radiative Prandtl number
T	Temperature
T_∞	Ambient temperature
T_w	Wall temperature
u	Velocity in x direction
υ	Velocity in y direction
c_p	Specific heat at constant pressure
θ	Similarity function for temperature
K	Permeability b of the porous medium
Q	Volumetric rate of heat generation
λ	Heat generation
N	Radiation on parameter
ρ	Density of the fluid
Ψ	Stream function

μ	Dynamic Viscosity
σ_1	Effective viscosity
σ_1	Stefan-Boltzman constant
κ_1	Absorption coefficient
η	Dimensionless similarity variable
v	Kinematic viscosity
∞	Free stream values
Re	Reynolds number

REFERENCES

[1] Sriramalu A, Kishan N and Anand RJ. Steady Flow and Heat Transfer of a Viscous Incompressible Fluid Flow through Porous Medium over a Stretching Sheet. J Energy Heat Mass Transfer 2001; 23: 483-495.

[2] Subhas A and Veena P. Visco-Elastic Fluid Flow and Heat Transfer in Porous Medium over a Stretching Sheet. Int J Non-Linear Mech 1998; 33: 531-540. http://dx.doi.org/10.1016/S0020-7462(97)00025-5

[3] Elbashbeshy EMA and Bazid MAA. Heat Transfer over a Continuously Moving Plate Embedded in a Non-Darcian Porous Medium. Int J Heat Mass Transfer 2000; 43: 3087-3092. http://dx.doi.org/10.1016/S0017-9310(99)00359-2

[4] Elbashbeshy EMA and Bazid MAA. Heat Transfer over an Unsteady Stretching Surface with Internal Heat Generation. Appl Math Comput 2003; 138(3): 239-245. http://dx.doi.org/10.1016/S0096-3003(02)00106-6

[5] Elbashbeshy EMA and Bazid MAA. Heat Transfer over a Stretching Surface with Internal Heat Generation. Can J Phys 2003, 81(4): 699-703. http://dx.doi.org/10.1139/p02-033

[6] Pop T and Na TY. Free Convection Heat Transfer of Non-Newtonian Fluids along a Vertical Wavy Surface in a Porous Medium. Proc 4th Int Symposium Heat Transfer 1996, Beijing, China; 452.

[7] He JH. Variational method a kind of non-linear analytical technique: some examples. Int J Non-Linear Mech 1999; 3414: 699-708. http://dx.doi.org/10.1016/S0020-7462(98)00048-1

[8] Adomian G. A review of the decomposition method and some recent results for nonlinear equation. Math Comput Model 1992; 13(7): 17. http://dx.doi.org/10.1016/0895-7177(90)90125-7

[9] Nayfeh AH. Perturbation methods. New York: Wiley; 2000. http://dx.doi.org/10.1002/9783527617609

[10] Ganji DD. The application of He's homotopy perturbation method to nonlinear equation arising in heat transfer. Physics letters A 2006; 355: 337-341. http://dx.doi.org/10.1016/j.physleta.2006.02.056

[11] Liao SJ. The proposed homotopy analysis technique for the solution of nonlinear problems. PhD Dissertation Shanghai Jiao Tong University; 1992.

[12] Liao SJ. Boundary element method for general nonlinear differential operators Eng Anal Bound Elem 1997; 202: 91-9. http://dx.doi.org/10.1016/S0955-7997(97)00043-X

[13] Liao SJ. An approximate solution technique not depending on small parameters: a special example. Int J Non-Linear Mech 1995; 303: 371-380. http://dx.doi.org/10.1016/0020-7462(94)00054-E

[14] Liao SJ. Beyond Perturbation: Introduction to the Homotopy Analysis Method. Chapman & Hall/CRC Press, Boca Raton 2003. http://dx.doi.org/10.1201/9780203491164

[15] Hayat T and khan M. Homotopy solutions for generalized second-grade fluid past porous plate. Nonlinear Dynamics 2005; 42: 395-405. http://dx.doi.org/10.1007/s11071-005-7346-z

[16] Fakhari A, Domairry G and Ebrahimpour. Approximate explicit solutions of nonlinear BBMB equations by homotopy analysis method and comparison with the exact solution. Phys Letter A 2007; 368: 64-8. http://dx.doi.org/10.1016/j.physleta.2007.03.062

[17] Rashidi MM, Domairry G and Dinarvand S. Solution of the laminar viscous flow in a semi-porous channel in the presence of a uniform magnetic field by using the homotopy analysis method. Commun Nonlinear Sci Numer Simulat 2007; 14: 708-717. http://dx.doi.org/10.1016/j.cnsns.2007.09.015

[18] Tan Y and Abbasbandy S. Homotopy analysis method for quadratic Riccati differential equation. Commun Nonlinear Sci Numer Simulat 2008; 13(3): 539-46. http://dx.doi.org/10.1016/j.cnsns.2006.06.006

[19] Domairry G and Fazeli M. Homotopy Analysis Method to Determine the Fin Efficiency of Convective Straight Fins with Temperature Dependent Thermal Conductivity. Communications in Nonlinear Science and Numerical Simulation 2009; 14(2): 489-499. http://dx.doi.org/10.1016/j.cnsns.2007.09.007

[20] Domairry G and Nadim N. Assessment of homotopy analysis method and homotopy perturbation method in non-linear heat transfer equation. International Communication Heat mass transfer 2008; 35(1): 93-102. http://dx.doi.org/10.1016/j.icheatmasstransfer.2007.06.007

[21] Ahmer M and Asif A. Analytic solution of generalized threedimensional flow and heat transfer over a stretching plane wall. Int Commun Heat Mass Transfer 2006; 33(10): 1243-1252. http://dx.doi.org/10.1016/j.icheatmasstransfer.2006.08.001

[22] Ghasemi E, McEligot DM, Nolan KP, Crepeau J, Tokuhiro A and Budwig RS. Entropy generation in a transitional boundary layer region under the influence of freestream turbulence using transitional RANS models and DNS. Int Comm Heat Mass Transf 2013; 41: 10-16. http://dx.doi.org/10.1016/j.icheatmasstransfer.2012.11.005

[23] Ghasemisahebi E. Entropy generation in transitional boundary layers. LAP LAMBERT Academic Publishing 2013.

[24] Ghasemi E, Soleimani S and Lin CX. Secondary reactions of turbulent reacting flows over a film-cooled surface. Int Com Heat Mass Transf 2014; 55: 93-101. http://dx.doi.org/10.1016/j.icheatmasstransfer.2014.04.007

[25] Ghasemi E, McEligot DM, Nolan KP, Crepeau J, Siahpush A, Budwig RS and Tokuhiro A. Effects of adverse and favorable pressure gradients on entropy generation in a transitional boundary layer region under the influence of freestream turbulence. Int J Heat Mass Transf 2014; 77: 475-488. http://dx.doi.org/10.1016/j.ijheatmasstransfer.2014.05.028

[26] Ghasemi E, Soleimani S, Barari A, Bararnia H and Domairry G. Influence of Uniform Suction/Injection on Heat Transfer of MHD Hiemenz Flow in Porous Media. J Eng Mech 2012; 138(1): 82-88. http://dx.doi.org/10.1061/(ASCE)EM.1943-7889.0000301

[27] Ganji DD, Bararnia H, Soleimani S and Ghasemi E. Analytical solution of the magneto-hydrodynamic flow over a nonlinear stretching sheet. Mod Phys Lett B 2009; 23: 2541-2556. http://dx.doi.org/10.1142/S0217984909020692

[28] Bararnia H, Ghasemi E, Soleimani S, Barari A and Ganji DD. HPM-Pade Method on Natural Convection of Darcian Fluid about a Vertical Full Cone Embedded in Porous Media. J Porous Media 2011; 14(6): 545-553. http://dx.doi.org/10.1615/JPorMedia.v14.i6.80

[29] Moghimi SM, Domairry G, Soleimani S, Ghasemi E and Bararnia H. Application of homotopy analysis method to solve MHD Jeffery–Hamel flows in non-parallel walls. Adv Eng Soft 2011; 42(3): 108-113. http://dx.doi.org/10.1016/j.advengsoft.2010.12.007

[30] Bararnia H, Ghasemi E, Soleimani S, Ghotbi AR and Ganji DD. Solution of the Falkner–Skan wedge flow by HPM–Pade' method. Adv Eng Soft 2012; 43(1): 44-52. http://dx.doi.org/10.1016/j.advengsoft.2011.08.005

[31] Jalaal M, Nejad MG, Jalili P, Esmaeilpour M, Bararnia H, Ghasemi E, Soleimani S, Ganji DD and Moghimi SM. Homotopy perturbation method for motion of a spherical solid particle in plane couette fluid flow. Comput Math Appl 2011; 61(8): 2267-2270. http://dx.doi.org/10.1016/j.camwa.2010.09.042

Received on 31-03-2015 Accepted on 20-04-2015 Published on 14-12-2015

DOI: http://dx.doi.org/10.15377/2409-5761.2015.02.02.2